Journal of Physics: Conference Series **205** (2010) 012044 doi:10.1088/1742-6596/205/1/012044

Fast timing: Lifetime measurements with $LaBr_3$ scintillators

I Deloncle[1], B Roussière[2], M A Cardona[3], D Hojman[3], J Kiener[1], P Petkov[4], D Tonev[4] and Ts Venkova[4]

[1]Centre de Spectrométrie Nucléaire et de Spectrométrie de Masse, CNRS/Université Paris-Sud XI, 91405 Orsay Campus,
[2]Institut de Physique Nucléaire,CNRS-IN2P3/Université Paris-Sud XI,
[3]Departamento de Fisica, CNEA, Buenos Aires, Argentina,
[4]Institue of Nuclear Research and Nuclear Energy, BAS, Sofia, Bulgaria.

E-mail: Isabelle.Deloncle@csnsm.in2p3.fr, roussier@ipno.in2p3.fr, cardona@tandar.cnea.gov.ar, hojman@tandar.cnea.gov.ar, petkov@inrne.bas.bg, Dimitar.Tonev@lnl.infn.it,venkova@inrne.bas.bg

Abstract. In order to perform half-life measurements at Alto, we developed a fast-timing set-up using fast scintillators : $LaBr_3$. The main components of our setup and their characteristics (timing properties) are presented. The resulting time resolution, obtained after optimization, and measured off-line with radioactive sources is discussed. This set-up was tested on-line by measuring using the slope method half-lives of $^{137-139}$Cs levels fed by the β^- decay of $^{137-139}$Xe. The neutron-rich Xe nuclei were produced by ^{238}U photofission using, at low intensity, the electron beam and the line of the future facility ALTO. Our results show the ability of such a fast-timing system to measure half-lives lower than the total time resolution. Off-line and on-line results are discussed.

1. Introduction

At the Orsay Tandem, the ALTO project [1] will soon open to nuclear structure studies a large number of exotic nuclei. This project consists in inducing the fission of ^{238}U by the photons emitted during the slowing down of an electron beam in a thick UC target (included in a MK5 ISOL target/source ensemble). The PARRNe-2 device is then used to separate the fragments that exited the source. The LEP-injector Linac has been settled at the Tandem in Orsay to provide the 50MeV electron beam at 10μA intensity. This will lead to a fission rate at ALTO of 10^{11} fission/s, comparable to the ones obtained at ISOLDE, OSIRIS and HRIB. With such a fission rate a large number of Lanthanide nuclei ($^{138-152}$La, $^{143-154}$Ce, $^{144-156}$Pr,$^{145-158}$Nd, $^{148-160}$Pm,$^{152-164}$Sm, $^{155-165}$Eu, $^{158-167}$Gd, $^{161-169}$Tb and $^{166-170}$Dy) [2] should be produced with a yield above 10 atoms per second, allowing, for some of them for the first time, decay spectroscopy to be performed. A lot of new interesting results are expected. Indeed, in this neutron-rich part of the lanthanide region a multitude of different phenomena are predicted, allowing to test our understanding of many nuclear physics aspects. For example, the p-n interaction, due to the orbitals involved, is expected to be strong and to give rise to very large deformation. Reciprocally, in this lanthanide region, a large number of 0^+ excited states are

observed that are not expected in deformed nuclei. The measurement of deformation of neutron-rich lanthanides is thus an important goal to be achieved that can be reached by determining the 2_1^+ lifetimes using the fast-timing method with $LaBr_3$ scintillators [3].

2. $LaBr_3$: detectors for direct lifetime measurements

Contrarily to indirect lifetime measurement methods, such as Doppler Shift Attenuation Method, that determine lifetimes from the Doppler shift (or/and the reshaping) of γ-ray lines emitted by recoiling nuclei – and require detectors with extremely good energy resolution –, the fast-timing method is the direct measurement of a time difference between two fast detector (scintillator) signals. The start is given when a populating transition of the interesting level is detected in one detector, and the stop when a deexciting transition of this level is detected in another detector. The determination of this time difference is limited by the time resolution of both detectors: start and stop signals should be well separated, identified as different moments. Therefore, as the decay of a quantum system level is governed by an exponential distribution toward high decay time (stop), lifetime below the time resolution of fast-timing set-u ps can be measured (cf section 6). Very good timing properties are not the only condition for fast-timing detectors. Indeed, the quality of the start and stop depends strongly on the quality of the populating and depopulating γ-ray energy selections and energy resolution is then also an important parameter for such a technique. The fast timing method, developed at first with BaF_2 detectors [4] knows nowadays a renewal with the recent discovery [5] of the $LaBr_3$ scintillators that present good properties on both time and energy response as presented in Table 1 and Table 2.

Table 1. Comparison of main properties of Ge and $LaBr_3$ detectors of same volume.

	Ge	$LaBr_3$
Energy range	keV to MeV	keV to MeV
Abs. Eff.(at 2,54cm from source)[6]	10^{-1} to 10^{-2}	2.10^{-1} to 5.10^{-2}
Rel. Eff. (@1.33MeV)	75%	143%
Energy resolution	1% to 1‰	20% to 3%
Typical time response	250 ns (risetime)	16ns (scint. decay time)
Time resolution	20 ns to 5ns [7]	200 ps(@511keV) [10, 11]

In Table 1 the main charateristics and the evolution of some properties for incident γ energy going from keV to MeV are compared for Ge and $LaBr_3$ crystals with the same volume (cylinders 3"x3"). One can first notice the very high efficiency of the $LaBr_3$ which is at least twice larger than the one of the Ge detector and nearly 40% greater than that of a NaI with the same volume. Moreover, the time resolution of $LaBr_3$ is enhanced by a factor of at least 25 compared to that of a Ge-detector, allowing to measure lifetime of the order of few tens of ps. Of course, Ge detectors are semiconductors and, even cooled to Nitrogen temperature, the gap between valence and conducting bands is small, inducing a high electron yield (300 per keV), and then impressive energy resolution – it goes as the inverse of the square root of the yield – of the order of ‰ at 1MeV. But, as it can be seen in Table 2 in which main properties of most popular scintillators are given (at room temperature), thanks to its high light yield, the $LaBr_3$ has a reasonable energy resolution, the best of the commonly used scintillators, ten times better in particular than that of BaF_2, which is the fastest scintillator nowadays. Nevertheless, the very short decay time of BaF_2 scintillation process (20 times better then for $LaBr_3$) does not fully profit to fast timing set-ups. First, the standard deviation in the timing distribution of the

photons emitted by scintillation is proportional to the ratio of the scintillation decay time to the light yield [8, 9], ratio which is then considered as the figure of Merit (F.o.M) of scintillators for timing measurements. From the similar F.o.M. values for BaF_2 and $LaBr_3$ crystals reported in Table 2, one can expect the same order of time resolution in fast-time measurements using either of them. Secondly, a fast-timing set-up includes an other stage of detection with a non neglectable intrinsic time resolution, contribution of which therefore will be reduced when dealing with large amount of particles (statistical reduction of the noise contribution).

Table 2. Comparison of main properties of common scintillators (data from [12] for BaF_2, from [13] for other crystals).

	$LaBr_3$	NaI(Tl)	BaF_2	BGO
Light Yield LY (ph./keV)	61	41	1.8	9
Decay time τ (ns)	16	250	0.7	300
F.O.M (τ/LY) [10]	0.26	6	0.38	33
Energy res. @662keV	2.7	5.6	11.4	9

3. Characteristics of Photomultipliers for fast-timing with $LaBr_3$

In scintillators incident gamma energy is converted in photons and not in electrons as in semi-conductors. A stage of conversion is then required in order to deal with an electric signal. This is performed by photomultipliers, which have non neglectable contribution to time resolution in fast-timing set-up.

A photomultiplier tube (PMT) consists in three different parts, gathered in one "tube". The conversion of photons to electrons, realized by photoelectric effect at the photocathode, has a limited quantum efficiency (QE), from 20% to 35% at 380 nm – the wavelength of $LaBr_3$ scintillation light –. The conversion is followed by electron collection which, due to geometrical and electron-optical factors of focusing electrodes, is only partial. Collected electrons are then transmitted to the multiplication part. It consists in several electrodes : a first dynode, accepting the largest amount of collected electrons; similar dynodes optimized for electron transmission between them; and the last dynode drawn to fit with the anode. The energy needed for secondary electron emission, in which one incident electron gives rise to δ (in mean) secondary electrons with lower energy, is provided (re-established) by an inter dynode potential.

Due to the different operations taking place in a PMT, the optimization of such a detector for applications requiring good energy and time resolutions, such as fast-timing, is very delicate and represents a difficult compromise. If the energy resolution is reduced by increasing the total number of electrons (statistics effect) at all operation, this is not true for the time resolution. Indeed, timing properties of a PMT are enhanced when most electrons have spent similar (short) times in the tube (i.e similar trajectories and speeds) and could be degraded if one enlarges the photocathode (or the collection efficiency, or the number of dynodes) without redrawing other components. As only two firms are making PMT development (Hamamatsu and Electron Tubes – Photonis PMT departement closed in July 2009), only few PMTs can be used for a fast-timing set-up.

Up to now we used, the XP2020 family PMTs [11]. Among them, the XP20D0 is used for $LaBr_3$. It has a borosilicate entry window and about 30% at 380 nm. The XP2020Q with a quartz window allowing UV light and about a QE 25% at 220 nm is more appropriate for BaF_2. In these PMTs, the improved collection between photocathode and first dynode

is associated with a new anode conception: an additional screening grid has been located in front of it [14], reducing the time jitter (time resolution). The time resolution measured with a light emitting diode for XP20D0 is between 220±13 ps and 260±13 ps [11], of the same order (250±1) for XP2020Q [15]. As already mentioned the intrinsic PMT time resolution is non negligible but for a scintillator+PMT association, the statistical effects due to the number of photoelectrons reduces the total time resolution. Indeed, it has been shown in ref.[11, 14] for $LaBr_3$ and BaF_2 respectively, that the product of total time resolution with the square root of the photoelectron number is constant, the value of the constant depending of the scintillator type (BaF_2, $LaBr_3$..). The total time resolution at 1.33MeV for a (⌀25x15mm) BaF_2/XP2020Q couple is 127 ps±5 (with 2300±80 Photoelectrons in the peak) [14], very near the 140 ps obtained for a (⌀25x25mm)$LaBr_3$/XP20D0 (with 17600±500 Phe)[11].

4. Configuration of the fast timing set-up

Two detectors are enough to define start and stop signals. Therefore, for levels populated in β decay, the start can be provided from β detection (for levels directly fed by β decay) or from γ-detection (with energy conditions). The stop can only be provided by the depopulating γ-ray detection. We developed then a fast timing set-up with three detectors: one plastic Pilot U scintillator (associated with a XP2020 PMT) for β-detection and two scintillating crystals (BaF_2 and $LaBr_3$ or two $LaBr_3$) for γ. The BaF_2 scintillator is associated with a XP2020Q PMT and the $LaBr_3$ are equiped with XP20D0 ones.

For each scintillator+PMT couple, the energy information entering the acquisition is made from the signal of the PMT last dynode, after amplification. The time information (a 'top' pulse) is built from the PMT anode signal using an analogical Constant Fraction Discriminator (CFD) module. In addition to the three 'reals' (E,T) channels, three others channels are defined for the time differences to be built : detector 1 for start with detector 2 as stop; detector 1 for start with detector 3 as stop; and detector 2 for start with detector 3 as stop. Indeed, the very good digitization step (400 ps) of the digital COMET card [16] entering the Orsay acquisition system, Narval [17], is too large compared to the expected time resolutions. The time differences signals have then to be obtained analogically before entering the acquisition system. Downstream CFDs, Time to Amplitude Converter (TAC) modules are used to deliver 'E'-like shaped signals in which the amplitudes are related to the time difference bewteen their two inputs (CFD outputs). Each analogical TAC output signal is then plugged as 'E', and its logical output is entered as 'T', in a virtual channel. In the following this 'E' information will be called TAC.

A large number of measurements, with different adjustements of the electronics, with different electronic modules and different detectors are needed to optimize such a fast timing set-up. For this reason, in the Narval acquisition user's program, we developed a new C module [18] allowing to get, on-line, multi-gated spectra. Many energy conditions (gates) can be imposed allowing for many different 'start' and 'stop' definitions in a same run, and half-lives for many levels to be observed simultaneously. For each possible combination of two gates, a double-gated TAC spectrum is built, incremented by 3(at least)-fold events consisting in the two selected energies (from two detectors), and the corresponding TAC information (between the two latter detectors). Any of such a spectrum can be displayed on the acquisition control window.

5. Optimization measurements with ^{60}Co source:

We performed many systematic measurements with a three detector configuration that allows time resolution of each detection channel to be obtained in a same run [19]. These measurements were performed with a ^{60}Co radioactive source, presenting only prompt concidences. We define gates set on the compton background as well as on the full energy peak in order to cover a large range of energies for the start and stop definitions. We first tested different electronic modules

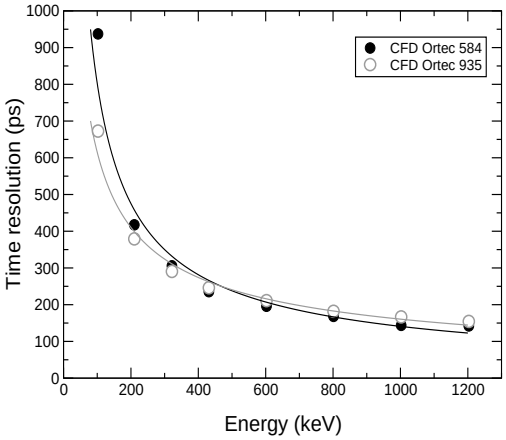

Figure 1. Time resolutions obtained for ⌀25,5x30 mm $LaBr_3$ crystal coupled to a XP20D0 PMT for two different CFDs as a function of energy.

(CFD, TAC) with different adjustments (High voltage applied on the PMT; Walk, external delay of the CFD). In fig.1 one can see the impressive time resolution improvement (200 ps less) at low energy (below 200keV) of a ⌀25,5x30 mm $LaBr_3$+XP20D0 PMT couple brought by the use of a 935 Ortec (empty squares) instead of a 584 Ortec (full square) CFD module.

For different scintillator+PMT detection couples we measured, as a function of the energy, energy and time resolution, absolute efficiency, linearity for several $LaBr_3$ scintillators. Indeed, the time resolution is strongly connected to crystal geometry and dimensions (see for example the recent work of ref.[20]). This is shown in fig.2 where are reported the time resolution curves obtained for two $LaBr_3$ cylindrical crystals with the same diameter (25,5 mm) but different lengthes (10 mm and 30 mm). For comparison, the time resolution curve obtained for the ⌀25,5x30 mm BaF_2 is also reported. A better time resolution (in mean 100 ps of improvement) is obtained with the smallest crystal for all the energy range, but it is more pronounced at low energy (around 200 ps). At the opposite, the peak to total ratio (see top spectrum of fig.3) is degraded in the small crystal due to bad high energy detection as compared to the one with the large one (bottom spectrum).

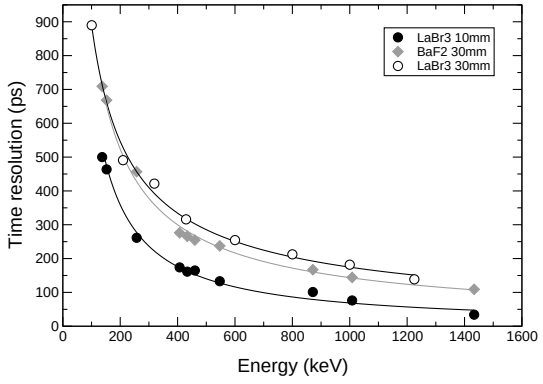

Figure 2. Time resolution obtained with a ⌀25,5x30 mm $LaBr_3$ (full line) and with a ⌀25,5x10 mm $LaBr_3$ (square), both coupled to XP20D0 PMT. For comparison is also reported the time resolution measured with a ⌀25,5x30 mm BaF_2+XP2020Q (square)

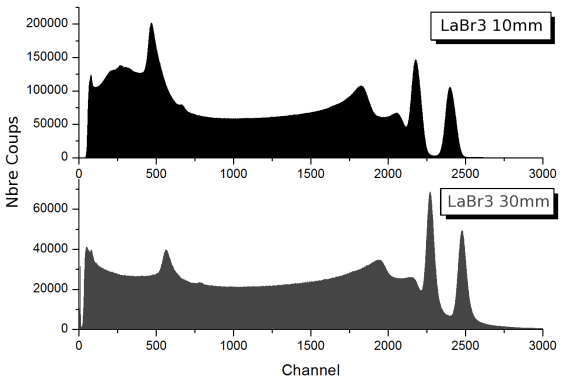

Figure 3. Energy spectra (^{60}Co source) obtained with the ⌀25,5x30 mm $LaBr_3$ (top spectrum) and with the ⌀25,5x10 mm $LaBr_3$ (bottom spectrum), both coupled to XP20D0 PMT.

6. Measurements at low intensity at ALTO:

In order to test on-line the performances of our fast timing set-up, we requested to use, at low intensity, the beam of the ALTO facility for measuring half-lives in $^{137-139}$Cs levels fed by the β^--decay of $^{137-139}$Xe. Indeed, if half-lives are known for levels up to nearly 450keV in ^{133}Cs, up to 250keV in ^{135}Cs, and, on the other side, up to 200keV in ^{141}Cs, none are known in the in between $^{137-139}$Cs isotopes. One half-life measurement has been carried out in ^{137}Cs using only two fast detectors (a plastic scintillator and a NaI crystal) [21], which lead to an upper limit of $T_{1/2} \leq 0.1$ ns for the first excited state. In the $^{133-139}$Cs isotopes the two first excited states are both $5/2^+$ states. The first one is originating from a $d_{5/2}$ quasiparticle excitation, the second from the coupling of 2_1^+ from the even core and one quasi-particle excitation from $1g_{7/2}$ – that leads to the $7/2^+$ ground state in all these isotopes. The decay of the $5/2_1^+$ to the ground state is then an l-forbiden transition but the half-lives for this state were expected to be less than or equal to 100 ps and of the order of 500 ps in $^{137-139}$Cs, respectively [22].

We performed the measurements last spring with the experimental set-up shown in fig.4. One can recognize in the top picture of fig.4, downwards, the tape station, the collection point, and the measurement point surrounded by the four detectors for the fast-timing setup: three scintillators, as previous, and one Ge that we added in order to increase our selectivity. The bottom picture is a zoom of this measurement point and shows counterclockwise : the ⌀25,4x3mm Pilot U, ⌀25,4x10 mm $LaBr_3$, and ⌀25,4x30 mm BaF_2), and the Ge detectors.

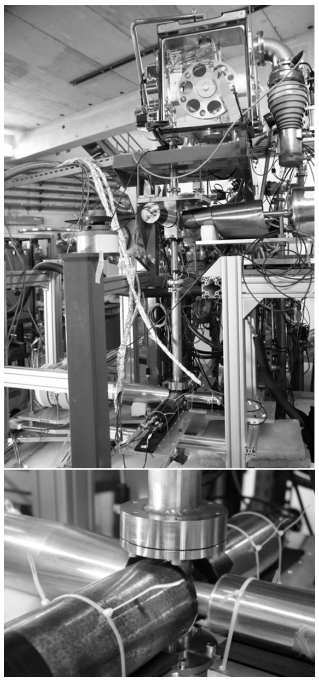

Figure 4. The 4-detector Fast-timing set-up used to measure half-lives at the ALTO beam line.

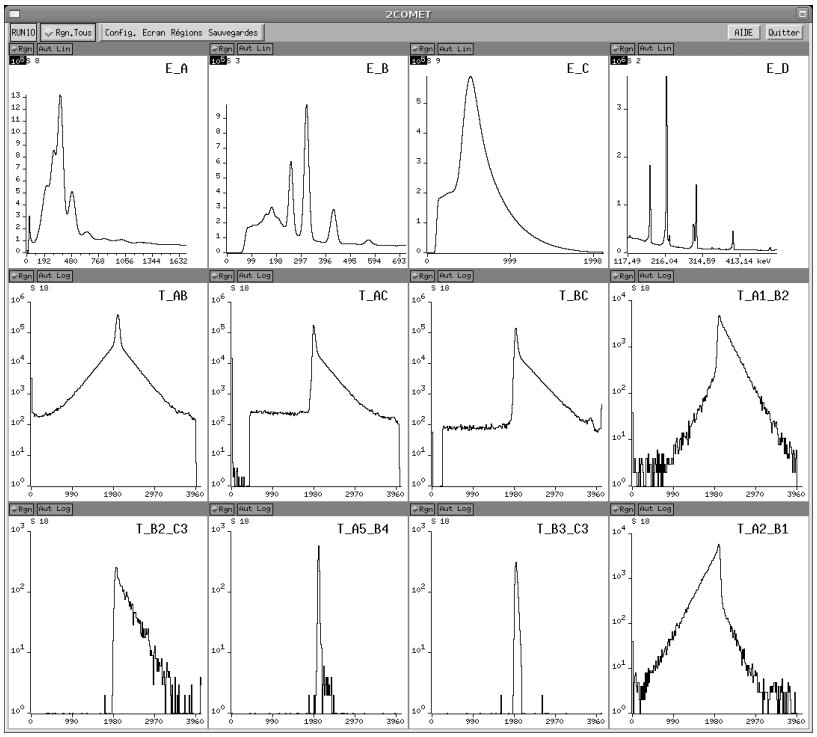

Figure 5. Picture of the Narval acquisition Spectrum Window. Direct Energy, TAC, as well as doubly gated TAC spectra obtained during the ^{139}Xe → ^{139}Cs run, are displayed.

As already mentioned, due to the implementation in the acquisition system Narval of multigating technique, we were able to observe on-line, during the experiment, the presence of some half-lives. A picture of the main window of the acquisition is presented Fig.5. On the first row one sees the energy spectra of the four detectors (A means BaF_2, B $LaBr_3$, C Pilot U and D Ge) and, on the second row the three total TAC spectra (no gates) (T_AB for the TAC between BaF_2 and $LaBr_3$, T_AC between BaF_2 and Pilot U, and between T_BC for Pilot U and $LaBr_3$). The following spectra are doubly gated TAC spectra. Their names T_Ai_Bj allow to recognize which gate (number between 1 to 5) was set on which detector (A to D) energy. The presence of a measurable half-life is easily recognizable in the T_A1_B2 (or T_A2_B1) spectrum, and in the T_B2_C3 one. They exhibit wide TAC, as compared for example to the narrow distribution observed in T_A5_B4 or T_B3_C3.

A preliminary analysis of the data allow us to attribute to the $5/2_1^+$ in ^{139}Cs the half-life of the T_A1_B2 spectrum and to estimate it, by the slope method, around 2.2ns. The Analysis is still in progress but the results are very promissing, half-lives below the time resolutions are already identified, lower than or of the order of 100 ps ($\pm$10 ps) for the levels at 289, 393 and 515 keV in ^{139}Cs.

Conclusions

A fast timing set-up has been developed for ALTO experiment. Its sensitivity in the range of few tens of picosecond to few nanosecond range has been recently established by the measurements of half-lives of $^{137-139}$Cs levels, that were populated in the decay of $^{137-139}$Xe isotopes produced at Alto by photofission.

Aknowledgement

This work was supported by the french Ministère des Affaires étrangères et européennes (ECO-NET program).

References

[1] S Essabaa, J Arianer, P Ausset, O Bajeat, J. P. Baronick *et al.* 2003 *Nucl. Inst. and Method.* B **204** 780
[2] B Roussière 2004 *Presentation to the ALTO Workshop*
`http://ipnweb.in2p3.fr/tandem-alto/alto/conferences/semin_pdf/roussiere.pdf`
[3] M A Cardona, D Hojman, B Roussière, I Deloncle *et al.* 2006 *Proposal to the Tandem Pac*
[4] H Mach, R L Gill and M Moszynski 1989 *Nucl. Inst. and Method.* A **280** 49
[5] E V D. Van Loef *et al.*, 2000 *Applied Physics Letter* **77** 1467
[6] J Kiener Geant simulation 2009 *private communication*
[7] C W Beausang et al. 1992 *Nucl. Inst. and Method.* A **204** 37
[8] R F Post and L I Schiff 1950 *Phys. Rev* **80** 1113
[9] A G Wright 2006 *Nucl. Phys.* B**150** 239
[10] Saint Gobain 2007 Technical Note
[11] M Moszynski *et al.* 2006 *Nucl. Inst. and Method.* B **567** 31
[12] Lawrence Berkeley Laboratory Scintillator Database *http://scintillator.lbl.gov/*
[13] O Sellès 2006 *Thèse de Doctorat de l'Université Paris VI*
[14] M Moszynski *et al.*, 2004 *Nucl. Sci. IEEE Trans.* **51** 1701
[15] M Moszynski *et al.*, 2005 *IEEE Trans. Nucl. Sci.* **52** 1027
[16] J Le Bris *et al.*, 2004 *Internal Report IPNO 05-04*
[17] J Le Bris, R Sellem, J C Artiges, J F Clavelin, S Du *et al.* 2006 *COMET-NARVAL ACQUISITION notice Rapport de recherche* 25 and http://hal.in2p3.fr/in2p3-00107358/fr/
[18] I Deloncle *to be published*
[19] J Pouthas *et al.* 1977 *Nucl. Inst. and Method.* **145** 445
[20] G Hull*et al.* 2008 *Nucl. Inst. and Method.* A **588** 384
[21] E Monnand *et al.*, 1975 *J. Physique* **36** 1.
[22] B Roussière *et al.* 2008 *Proposal to the Tandem Pac*